Thermodynamic properties of extremely diluted symmetric Q-Ising neural networks

2000 J. Phys. A: Math. Gen. 33 6481

(http://iopscience.iop.org/0305-4470/33/37/302)

J. Phys. A: Math. Gen. **33** (2000) 6481–6495. Printed in the UK PII: S0305-4470(00)12072-4

Thermodynamic properties of extremely diluted symmetric Q-Ising neural networks

D Bollé†§, D M Carlucci† and G M Shim‡

† Instituut voor Theoretische Fysica, KU Leuven, B-3001 Leuven, Belgium

‡ Department of Physics, Chungnam National University, Yuseong, Taejon 305-764, Korea

E-mail: desire.bolle@fys.kuleuven.ac.be, domenico.carlucci@fys.kuleuven.ac.be and gmshim@cnu.ac.kr

Received 16 February 2000

Abstract. Using the replica-symmetric mean-field theory approach the thermodynamic and retrieval properties of extremely diluted *symmetric* Q-Ising neural networks are studied. In particular, capacity–gain parameter and capacity–temperature phase diagrams are derived for $Q = 3$, 4 and ∞. The zero-temperature results are compared with those obtained from a study of the dynamics of the model. Furthermore, the de Almeida–Thouless line is determined. Where appropriate, the difference from other Q-Ising architectures is outlined.

1. Introduction

Recently the dynamics of extremely diluted *symmetric* Q-Ising neural networks has been solved completely [1]. In spite of the extreme dilution, it is the symmetry that causes feedback correlations from the second time step onwards, in contrast with an asymmetric architecture [2, 3], complicating the dynamics in a nontrivial way. Based upon the time evolution of the distribution of the local field a recursive scheme has been developed in order to calculate the evolution of the relevant order parameters of the network at zero temperature. Furthermore, by requiring that the local field becomes time independent, implying that some correlations are neglected, fixed-point equations are obtained and the capacity–gain parameter phase diagrams for the $Q = 2$, 3 models have been discussed briefly.

For the case of $Q = 2$ it turns out that the resulting fixed-point equations from this dynamic approach are the same as those derived from a thermodynamic replica-symmetric mean-field theory treatment given in [4]. This gives us some insight concerning a possible relation between replica symmetry and the structure of the noise. Of course, it would be interesting to know whether this stays valid for $Q > 2$. Besides, a detailed discussion of the phase diagram for these extremely diluted symmetric models is interesting on its own. However, for these cases a thermodynamic approach is not yet available in the literature. The purpose of this work is precisely to present the results of such an approach.

Concretely, we consider the extremely diluted symmetric Q-Ising neural network with arbitrary gain parameter. Using the replica-symmetric mean-field approximation we investigate both its thermodynamic and retrieval properties at zero and non-zero temperatures. Explicit results are presented for $Q = 3$, 4 and ∞.

§ Also at Interdisciplinair Centrum voor Neurale Netwerken, KU Leuven, Belgium.

0305-4470/00/376481+15$30.00

The rest of this paper is organized as follows. In section 2 the model is introduced from a dynamical point of view. Section 3 presents the replica-symmetric mean-field approximation and obtains the relevant fixed-point equations for general Q. In section 4 these equations are studied in detail for arbitrary temperatures and $Q = 3$ (section 4.1), 4 (section 4.2) and ∞ (section 4.3). In particular, the storage capacity as a function of the gain parameter and capacity–temperature phase diagrams are obtained. The specific thermodynamic properties are discussed. The results turn out to be significantly different for odd and even Q. They are compared with those for other architectures of these Q-Ising models. Section 5 presents the concluding remarks. Finally, the appendix contains the specific fixed-point equations for the different values of Q treated in the paper.

2. The model

Consider a network of N neurons which can take values σ_i in the set of equidistant states

$$\mathcal{S}_Q = \{s_k = -1 + 2(k-1)/(Q-1), k = 1, \ldots, Q\}. \tag{1}$$

In this network we want to store p patterns $\{\boldsymbol{\xi}^\mu, \mu = 1, \ldots, p\}$ that are supposed to be independent and identically distributed random variables (IIDRVs) with zero mean and variance A. The latter is a measure for the activity of the patterns.

Given a configuration $\boldsymbol{\sigma} = (\sigma_1, \ldots, \sigma_N)$, the local field h_i of neuron i is

$$h_i(\boldsymbol{\sigma}) = \sum_{j \neq i} J_{ij}\sigma_j \tag{2}$$

with J_{ij} the synaptic couplings between neurons i and j.

The network is taken to be extremely diluted but symmetric, meaning that the couplings are chosen as follows. Let $\{c_{ij} = 0, 1\}, i, j = 1, \ldots, N$ be IIDRVs with distribution $\Pr\{c_{ij} = x\} = (1 - c/N)\delta_{x,0} + (c/N)\delta_{x,1}$ and satisfying $c_{ij} = c_{ji}$, $c_{ii} = 0$, then

$$J_{ij} = \frac{c_{ij}}{Ac} \sum_{\mu=1}^{p} \xi_i^\mu \xi_j^\mu \qquad \text{for} \quad i \neq j. \tag{3}$$

We remark that compared with the asymmetrically diluted model [3] the architecture is still a local Cayley tree but no longer directed. In the limit $N \to \infty$ the probability that the set of connections, $T_i = \{j = 1, \ldots, N | c_{ij} = 1\}$, giving information to the site i, is equal to a certain number k remains a Poisson distribution with mean $c = E[|T_i|]$. Thereby it is assumed that $c \ll \log N$. In order to obtain an infinite average connectivity allowing us to store infinitely many patterns p, one also takes then the limit $c \to \infty$ and defines the capacity α by $p = \alpha c$. However, although for the asymmetric architecture, at any given time step t all spins are uncorrelated and hence no feedback is present, for the symmetric architecture this is no longer the case, causing feedback from $t \geqslant 2$ onwards [5,6]. Indeed, if the coupling J_{ij} is non-zero then J_{ji} is also non-zero and therefore the state of neuron i at time t depends on its state at time $t-2, t-4, \ldots$. This is not the case for asymmetric dilution since the probability of having a non-zero J_{ji}, given a non-zero J_{ij}, vanishes.

The neurons are updated asynchronously according to the transition probability

$$\Pr(\sigma_i' = s_k | \boldsymbol{\sigma}) = \frac{\exp[-\beta\epsilon_i(s_k|h_i(\boldsymbol{\sigma}))]}{\sum_{l=1}^{Q} \exp[-\beta\epsilon_i(s_l|h_i(\boldsymbol{\sigma}))]}. \tag{4}$$

Here the inverse temperature $\beta = T^{-1}$ measures the noise level, and the energy potential $\epsilon_i(s|h)$ is taken to be [7]

$$\epsilon_i(s|h) = -hs + bs^2 \qquad b > 0. \tag{5}$$

At zero temperature, σ_i' takes the value s_k leading to the minimum of the energy potential. This is equivalent to using an input–output relation

$$\begin{aligned} \sigma_i' &= g_b[h_i(\boldsymbol{\sigma})] \\ g_b(x) &= \sum_{k=1}^{Q} s_k[\theta(b(s_{k+1}+s_k)-x)-\theta(b(s_k+s_{k-1})-x)] \end{aligned} \tag{6}$$

with $s_0 = -\infty$ and $s_{Q+1} = \infty$. For finite Q this input–output relation has a steplike shape and the parameter b controls the steepness of the steps. For $Q = \infty$ the input–output function (6) becomes the piecewise linear function

$$g_b(x) = \begin{cases} \operatorname{sign}(x) & \text{if} \quad |x| > 2b \\ \dfrac{x}{2b} & \text{otherwise.} \end{cases} \tag{7}$$

The slope of the linear part is given by $(2b)^{-1}$. In general, as b goes to zero the input–output relation reduces to that of the Ising-type network independent of Q.

In what follows we present a detailed study of the properties of these symmetrically diluted networks as a function of T and b.

3. Replica-symmetric mean-field theory

The long-time behaviour of the network under consideration is governed by the Hamiltonian

$$H = -\tfrac{1}{2}\sum_{i\neq j} J_{ij}\sigma_i\sigma_j + b\sum_i \sigma_i^2. \tag{8}$$

In order to calculate the free energy we use the standard replica method as applied to dilute spin-glass models [4, 8–10]. Starting from the replicated partition function averaged over the connectivity and the non-condensed patterns we arrive at

$$\langle \mathcal{Z}^n \rangle_c = \prod_{\mu,\gamma}\left[\int \mathrm{d}m_\gamma^\mu\right]\prod_{\gamma,\gamma'}\left[\int \mathrm{d}q_{\gamma\gamma'}\right]\prod_{\gamma}\left[\int \mathrm{d}\tilde{q}_\gamma\right]\exp[-N\beta f] \tag{9}$$

$$f = \frac{A}{2}\sum_{\mu,\gamma}(m_\gamma^\mu)^2 + \frac{\beta\alpha}{2}\sum_{\gamma<\gamma'} q_{\gamma\gamma'}^2 + \frac{\beta\alpha}{2}\sum_\gamma \tilde{q}_\gamma^2 - \frac{1}{\beta}\langle\langle \ln_{\{\sigma^\alpha\}} \operatorname{Tr}\exp[-\beta\tilde{H}]\rangle\rangle_{\{\xi\}} \tag{10}$$

$$\tilde{H} = -\sum_{\mu,\gamma} m_\gamma^\mu \xi^\mu \sigma_\gamma - \beta\alpha\sum_{\gamma<\gamma'} q_{\gamma\gamma'}\sigma_\gamma\sigma_{\gamma'} + \sum_\gamma\left(b - \frac{\alpha\beta}{2}\tilde{q}_\gamma\right)\sigma_\gamma^2 \tag{11}$$

where m_γ^μ, $q_{\gamma\gamma'}$, $\tilde{q}_\gamma$ are the usual order parameters defined by

$$m_\gamma^\mu = \frac{1}{N}\sum_i \xi_i^\mu \langle\sigma_{\gamma,i}\rangle \qquad \gamma = 1,\ldots,n \tag{12}$$

$$q_{\gamma\gamma'} = \frac{1}{N}\sum_i \langle\sigma_{\gamma,i}\rangle\langle\sigma_{\gamma',i}\rangle \qquad \gamma \neq \gamma' = 1,\ldots,n \tag{13}$$

$$\tilde{q}_\gamma = \frac{1}{N}\sum_i \langle\sigma_{\gamma,i}^2\rangle \qquad \gamma = 1,\ldots,n \tag{14}$$

with n the number of replicas and the sum over μ running over the number of condensed patterns s. Assuming replica symmetry, i.e. $m_\gamma^\mu = m_\mu, q_{\gamma\gamma'} = q, \tilde{q}_\gamma = \tilde{q}$ the, free energy becomes

$$\begin{aligned} f(\beta) = \lim_{n\to 0}\frac{f}{n} &= \frac{A}{2}\sum_\mu (m_\mu)^2 + \frac{\alpha}{4\beta}\chi^2 + \frac{\alpha}{2}q\chi \\ &\quad -\frac{1}{\beta}\left\langle\!\!\left\langle \int \mathcal{D}z \ln_{\{\sigma\}} \operatorname{Tr}\exp\left[\beta\sigma\left(\sum_\mu m_\mu\xi^\mu + \sqrt{\alpha q}z - \tilde{b}\sigma\right)\right]\right\rangle\!\!\right\rangle_{\{\xi\}} \end{aligned} \tag{15}$$

with $\tilde{b} \equiv b - \frac{\alpha}{2}\chi$ the effective gain parameter, $\chi \equiv \beta(\tilde{q} - q)$ the susceptibility and $\mathcal{D}z = \mathrm{d}z\,(2\pi)^{-1/2}\exp(-z^2/2)$ the Gaussian measure. We remark that the effective gain parameter $\tilde{b}$ can be negative, implying that the input–output function reduces to that of 2-Ising-type neurons, i.e. $g_{\tilde{b}}(h) = \mathrm{sign}(h)$. Furthermore, we note that the free energy (15) can be obtained as the *formal* expansion to second order in χ of the free energy for the fully connected model derived in [11].

The phase structure of the network is determined by the solution of the fixed-point equations for the order parameters

$$m_\mu = \frac{1}{A}\left\langle\!\!\left\langle \int \mathrm{D}z\,\xi^\mu \langle\sigma(z)\rangle \right\rangle\!\!\right\rangle \tag{16}$$

$$q = \left\langle\!\!\left\langle \int \mathrm{D}z\,\langle\sigma(z)\rangle^2 \right\rangle\!\!\right\rangle \tag{17}$$

$$\chi = \frac{1}{\sqrt{\alpha q}}\left\langle\!\!\left\langle \int \mathrm{D}z\,z\langle\sigma(z)\rangle \right\rangle\!\!\right\rangle \tag{18}$$

which extremize $-\beta f(\beta)$. Here

$$\langle\sigma(z)\rangle = \frac{\mathrm{Tr}_\sigma\,\sigma\exp\left[\beta\sigma\left(\sum_\mu m_\mu\xi^\mu + \sqrt{\alpha q}z - \tilde{b}\sigma\right)\right]}{\mathrm{Tr}_s\exp\left[\beta s\left(\sum_\mu m_\mu\xi^\mu + \sqrt{\alpha q}z - \tilde{b}s\right)\right]}. \tag{19}$$

In the following section we discuss these equations for $Q = 3, 4$ and ∞ models.

4. Thermodynamic and retrieval properties

4.1. $Q = 3$

In the rest of this work we are mainly interested in the Mattis retrieval state, so we consider one condensed pattern, say the first one. Then we can write $m_\mu = m\delta_{\mu 1}$ and, furthermore, we leave out the index 1 in the following.

Let us consider a three-state network with uniformly distributed patterns taking the values $0, \pm 1$ such that $A = 2/3$. For the Mattis retrieval state the average (19) is given by

$$\langle\sigma(z)\rangle = \frac{\sinh\left[\beta\left(m\xi + \sqrt{\alpha q}z\right)\right]}{\frac{1}{2}\exp(\beta\tilde{b}) + \cosh\left[\beta\left(m\xi + \sqrt{\alpha q}z\right)\right]} \tag{20}$$

which reads at zero temperature

$$\langle\sigma(z)\rangle = g_{\tilde{b}}\left(m\xi + \sqrt{\alpha q}z\right). \tag{21}$$

The fixed-point equations (16)–(18) can then easily be written down and the integration can be performed explicitly at zero temperature. For completeness we present them in the appendix.

First we look at the network at zero temperature. For $\tilde{b} \leqslant 0$ these fixed-point equations can be further reduced by taking the limit $\tilde{b} \to 0$ and introducing the variable $x = m/\sqrt{2\alpha q}$. One arrives at

$$\sqrt{2\alpha} = \frac{\mathrm{erf}(x)}{x} \tag{22}$$

with, in view of the definition of $\tilde{b} = b - \frac{\alpha}{2}\chi$,

$$b \leqslant b_0 = \sqrt{\frac{\alpha}{18\pi}}[2\exp(-x^2) + 1]. \tag{23}$$

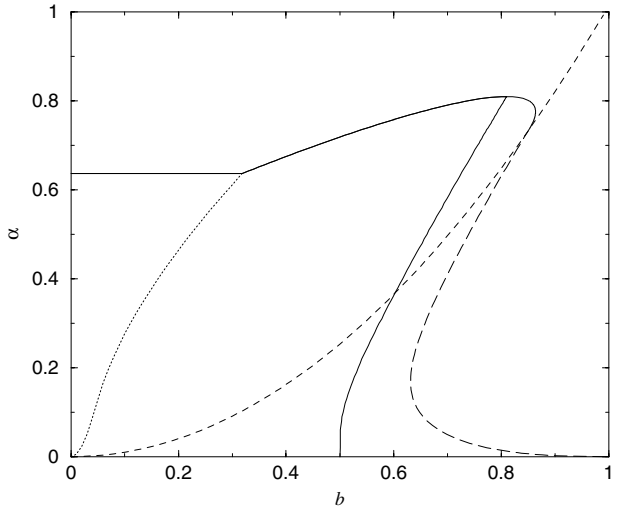

Figure 1. $Q = 3$ α–b phase diagram for uniform patterns at $T = 0$. The (thin) full and long-dashed curves denote the boundary of the retrieval region corresponding respectively to a continuous and discontinuous appearance of the solution. The dotted line separates the 2-Ising-like retrieval region. The short-dashed curve indicates the discontinuous appearance of the spin-glass state. The thick full curve represents the thermodynamic transition for the retrieval state.

This teaches us that the retrieval state vanishes continuously at $\alpha_c = 2/\pi$ for $b \leqslant b_0 = 1/\pi$.

The phase boundary of the retrieval state for $\tilde{b} > 0$ can be obtained by numerically solving the fixed-point equations (A5)–(A7). The results are shown in the capacity–gain parameter phase diagram presented in figure 1 as the full and the long-dashed curve. The full curve denotes a continuous appearance of the retrieval state, the long-dashed curve a discontinuous one. Furthermore, the dotted curve separates the 2-Ising-like region (which is to the left) where $\tilde{b} \leqslant 0$.

Finally, the short-dashed curve in this diagram indicates the boundary above which the spin-glass solution exists. The spin glass is characterized by taking $m = 0$ and $q \neq 0$ in (A5)–(A7). The resulting fixed-point equations can be combined into a single equation in the variable $y = \tilde{b}/\sqrt{2\alpha q}$

$$\frac{b}{\sqrt{2\alpha}} = y\sqrt{1 - \operatorname{erf}(y)} + \frac{\exp(-y^2)}{2\sqrt{[\pi(1 - \operatorname{erf}(y))]}}. \tag{24}$$

Since the right-hand side of the above equation is bounded, a spin-glass solution is possible when $\alpha \geqslant cb^2$ with $c \approx 1.0134$. It vanishes discontinuously at the boundary.

In order to find the thermodynamic transition line we have to determine which state—retrieval, spin glass or paramagnetic—leads to the lowest free energy. At zero temperature the free energy is given by

$$f = -\frac{A}{2}m^2 - \frac{\alpha}{2}q\chi + \tilde{b}q \tag{25}$$

as long as χ is finite. This is certainly the case when q is nonzero. Since also $q = 0$ for the paramagnetic state, however, it is necessary to check whether χ is finite. The paramagnetic state is determined by the equation

$$\tilde{b} = b - \frac{\alpha\beta}{\exp(\beta\tilde{b}) + 2}. \tag{26}$$

This equation has three solutions. In the limit $T \to 0$, only the solution that converges to b with $\chi \sim 2\beta \exp(-\beta b) \to 0$ is stable against longitudinal fluctuations as is easily seen by expanding the free energy for small q. The free energy of this stable paramagnetic state is always zero. The retrieval state becomes the global minimum of the free energy in the region bounded by the thick full curve. So, for $\alpha = 0$ the retrieval state is the minimum for $b \in [0, 1/2]$. The latter is true independent of the architecture. To the right of the thick full curve the paramagnetic state is the global minimum. We remark that this paramagnetic state at $T = 0$ is in fact simply a frozen state with all the spins taking the value zero (and not a phase where all the spins take all possible values with the same probability).

Finally, the stability of the replica symmetric retrieval solution against replica-symmetry breaking is determined by the replicon eigenvalue [12]

$$\lambda_R = 1 - \beta^2 \alpha \left\langle\!\!\left\langle \int \mathcal{D}z (\langle \sigma^2(z) \rangle - \langle \sigma(z) \rangle^2)^2 \right\rangle\!\!\right\rangle_{\{\xi\}} \tag{27}$$

$$= 1 - \frac{1}{q} \left\langle\!\!\left\langle \int \mathcal{D}z (\partial_z \langle \sigma(z) \rangle)^2 \right\rangle\!\!\right\rangle_{\{\xi\}} \tag{28}$$

where $\langle \sigma(z) \rangle$ is given by equation (20). In the limit $T \to 0$, $\langle \sigma(z) \rangle$ becomes a step function so the argument of the integration over z is proportional to the square of the delta function. Therefore the replicon eigenvalue for the retrieval solution at $T = 0$ is always negative and, hence, replica symmetry is broken.

For the paramagnetic solution that we have discussed before we find that the replicon eigenvalue $\lambda_{PM} = 1$ so that this state is also stable against transverse fluctuations.

At this point a couple of remarks are in order. First, we note that the fixed-point equations and, hence, also the α–T phase diagram are precisely the same as those obtained from an exact dynamical approach (see [1] equations (23)–(25) and figure 2) after requiring that the evolution of the distribution of the local field becomes stationary at a certain time t. This requirement has the consequence that most of the discrete noise caused by the feedback in the retrieval dynamics is neglected. It would mean that for these models a replica-symmetric mean-field theory treatment corresponds to a specific simplification of the structure of the noise—only the Gaussian part plus the discrete noise from the last time step—induced by the non-condensed patterns. This is also related to the so called self-consistent signal-to-noise-ratio analysis introduced in [13]. However, more work is needed, also on other models, to put such a type of conjecture on a firm basis. Second, it is interesting to compare the phase diagram figure 1 with the one for the extremely diluted *asymmetric* architecture [3]. The essential difference is that the 2-Ising-like region is much more extended here. The rest of the diagram has, in fact, a similar shape but it is tilted because of this Ising-like region towards greater b-values (compare [3] figure 1).

Next we consider the $Q = 3$ network at non-zero temperatures. The results are presented in figures 2 and 3. From $T = 0.37$ onwards the retrieval state appears continuously at the whole boundary. Furthermore, the retrieval state is the global minimum of the free energy in a growing region covering the whole retrieval region of the phase diagram as the temperature increases to $T = 0.5$. For $T = 0.6$ the lower branch of the retrieval boundary ends in zero such that for higher temperatures we apparently have no retrieval for small values of α. For $T = 0.7$ and $b = 0$, e.g., $\alpha \geqslant 0.2$. Finally, the replica symmetry solution is no longer unstable in the whole retrieval region. Calculating the replicon eigenvalue (28) leading to the de Almeida–Thouless (AT) line (dashed–dotted curve in figures 2 and 3), we find a growing region of stability in the phase diagram below this AT line.

In order to give a more complete idea of these results we present the capacity–temperature phase diagrams in figure 3. We immediately notice that for higher temperatures we obtain a

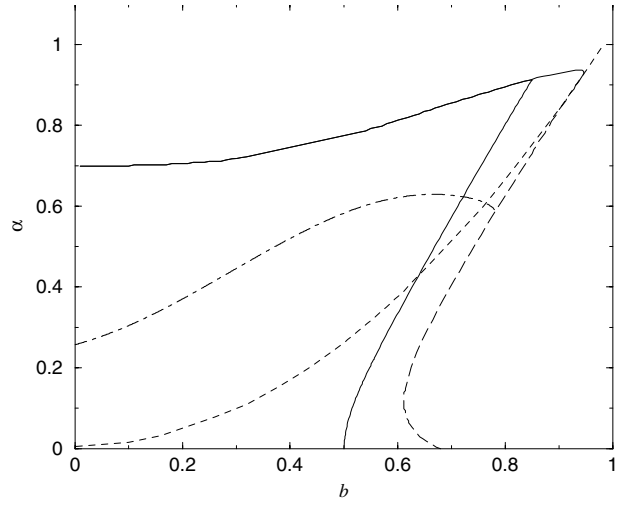

(*a*)

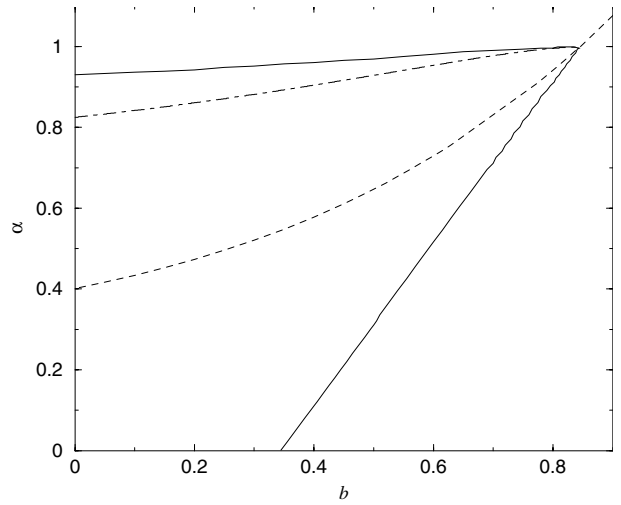

(*b*)

Figure 2. $Q = 3$ α–b phase diagram for uniform patterns at (*a*) $T = 0.1$ and (*b*) 0.5. The meaning of the curves is as in figure 1. The dashed–dotted curve is the de Almeida–Thouless line, above which replica symmetry is unstable.

higher critical capacity, in other words the upper branch of the retrieval boundary shows some strong re-entrant behaviour. This is not surprising since this branch lies completely in the region where replica symmetry is broken, in contrast with the fully connected (symmetric) model [11]. It is common knowledge, at least for $Q = 2$ [4, 8], that re-entrance is due to the use of the replica-symmetric approximation. It is also conjectured there that a full replica-symmetry-breaking solution might be a horizontal line above this upper branch of the retrieval boundary starting from the high-temperature point. Validating this conjecture by numerical simulations or performing a one-step replica-symmetry-breaking calculation in order to see whether such results lie indeed closer to this horizontal line are beyond the scope of the present work.

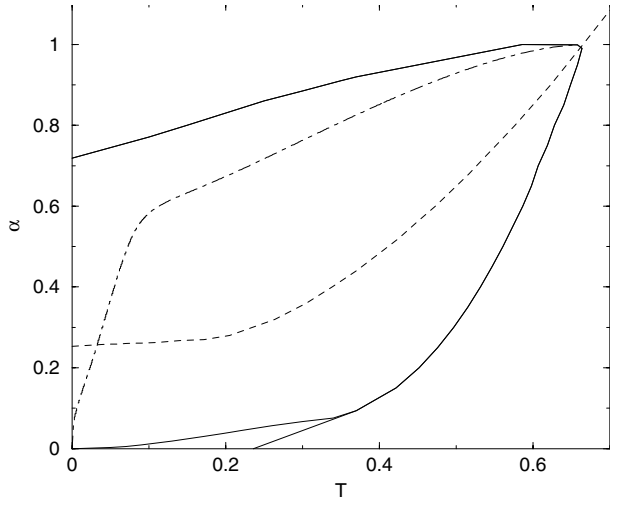

(*a*)

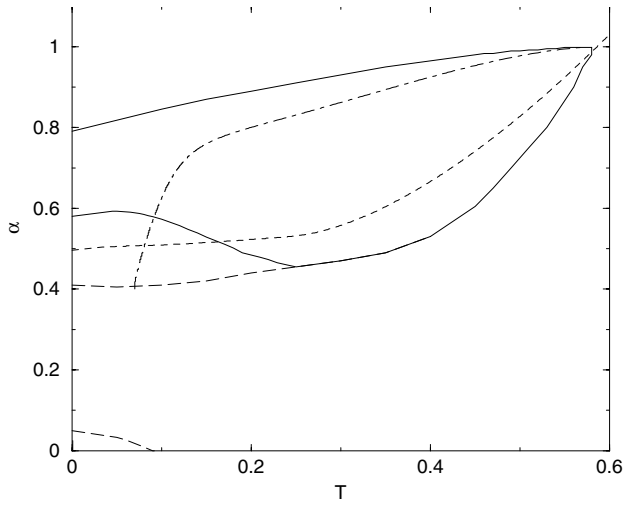

(*b*)

Figure 3. $Q = 3$ α–T phase diagrams for uniform patterns and (*a*) $b = 0.5$ and (*b*) 0.7. The meaning of the lines is as in figures 1 and 2.

4.2. $Q = 4$

The thermodynamic properties of a network consisting of neurons that are able to take on the zero state ($\sigma_i = 0$) are significantly different from those of a network in which this state is forbidden for the neurons. Indeed, for the even-Q models a paramagnetic phase at zero temperature has to be absent precisely because the spins cannot take the value zero and, hence, q cannot be zero physically. For high temperatures, of course, q can be zero and such a phase does exist. This is similar to the asymmetric diluted architecture [3] and the fully connected architecture [11]. As a representative example we consider the $Q = 4$ model in this section.

According to (1) the neurons, as well as the patterns, can take on the values

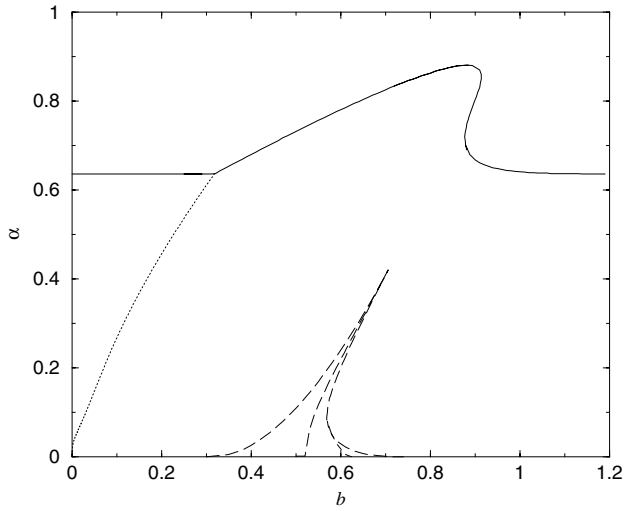

Figure 4. $Q = 4$ α–b phase diagrams for uniform patterns at $T = 0$. The meaning of the curves is as in figure 1. The triangular region is explained in the text.

$-1, -1/3, +1/3, +1$. We consider uniformly distributed patterns so that $A = 5/9$.

At zero temperature, the fixed-point equations for a retrieval state with $\tilde{b} > 0$ are given in the appendix. For $\tilde{b} < 0$, these equations can be further reduced by the introduction of the variable $x = m/\sqrt{2\alpha q}$ to

$$\sqrt{2\alpha} = \frac{9}{10x}\left[\operatorname{erf}(x) + \frac{1}{3}\operatorname{erf}\left(\frac{1}{3}x\right)\right] \tag{29}$$

with, in view of the definition of $\tilde{b}$

$$b \leqslant b_0 = \sqrt{\frac{\alpha}{8\pi}}\left[\exp(-x^2) + \exp\left(-\frac{1}{9}x^2\right)\right]. \tag{30}$$

Exactly as in the $Q = 3$ case the retrieval state vanishes continuously at $\alpha_c = 2/\pi$ for $b \leqslant b_0 = 1/\pi$. In contrast with $Q = 3$, however, the fixed-point equations have retrieval solutions for all values of b. When $b \to \infty$, they can also be reduced to a single equation similar to equation (29). This means that the retrieval state again vanishes continuously at $\alpha_c = 2/\pi$. For the other values of b the retrieval phase boundary can be obtained numerically from (A8)–(A10). The result is indicated in figure 4 by a full curve expressing the fact that the retrieval state appears continuously everywhere.

The triangular region in figure 4 bordered by the thin long-dashed curve indicates the existence of two retrieval states with different free energies. Both stable retrieval states have the same free energies at the thick long-dashed curves. In order to obtain an idea of the relevant b- and m-values for this case, we note that for $\alpha = 0$

$$\begin{aligned} b < 1/4 \quad &: \quad m = 6/5 \\ 1/4 < b < 3/10 \quad &: \quad m = 6/5 \text{ and } 1 \\ 3/10 < b < 3/4 \quad &: \quad m = 1 \text{ and } 2/5 \\ 3/4 < b \quad &: \quad m = 2/5 \end{aligned} \tag{31}$$

Again, these results are valid independent of the architecture (cf [3, 11]).

Concerning the spin-glass states we have to solve the equations (A8)–(A10) for $m = 0$. It is straightforward to check that a spin-glass phase exists in the whole region of the phase diagram. By looking at the free energy expression (25) we find that it is always energetically unfavourable versus the retrieval state (only versus the one with the lower free energy when there are two). Furthermore, the retrieval state is unstable against replica symmetry breaking.

Comparing the phase diagram of the $Q = 4$ model with that of the asymmetrically diluted model [3] we see that, similar to the $Q = 3$ case, there is an extended 2-Ising-like region here. Again the overall shape is similar apart from the fact that it is tilted towards greater b-values (cf [3] figure 4).

4.3. $Q = \infty$

Finally we turn to the case $Q = \infty$. Considering again uniformly distributed patterns between -1 and 1 (and hence $A = 1/3$) the fixed-point equations are still given by (16)–(18) with (19) replaced by

$$\langle \sigma(z) \rangle = \frac{\int_{-1}^{1} \mathrm{d}\sigma\, \sigma \exp\left[\beta\sigma\left(\sum_\mu m_\mu \xi^\mu + \sqrt{\alpha r} z - \tilde{b}\sigma\right)\right]}{\int_{-1}^{1} \mathrm{d}s \exp\left[\beta s\left(\sum_\mu m_\mu \xi^\mu + \sqrt{\alpha r} z - \tilde{b} s\right)\right]}. \tag{32}$$

For the retrieval state at zero temperature this leads to the explicit fixed-point equations presented in (A11)–(A13) of the appendix. These equations are written down for $\tilde{b} > 0$. Again, for $\tilde{b} \leqslant 0$ the equations can be further reduced by introducing the variable $x = m/\sqrt{2\alpha q}$:

$$\sqrt{2\alpha} = \frac{3}{2}\left[\frac{\mathrm{erf}(x)}{x}\left(1 - \frac{1}{2x^2}\right) + \frac{1}{\sqrt{\pi} x^2}\exp(-x^2)\right] \tag{33}$$

together with, in view of the definition of $\tilde{b}$, the following condition:

$$b \leqslant b_0 = \sqrt{\frac{\alpha}{8}}\frac{\mathrm{erf}(x)}{x}. \tag{34}$$

Exactly as in the $Q = 3$ and 4 model, these equations tell us that the retrieval state vanishes continuously at $\alpha_c = 2/\pi$ for $b \leqslant b_0 = 1/\pi$. In fact, one can analytically show that the critical boundary of this 2-Ising-like region is independent of Q. Indeed, in this region the general fixed-point equations (16)–(19) at $T = 0$ together with the condition $\tilde{b} \leqslant 0$ lead to

$$\sqrt{2\alpha} = \frac{1}{Ax}\langle\langle \xi\, \mathrm{erf}(x\xi)\rangle\rangle \tag{35}$$

$$b \leqslant \sqrt{\frac{\alpha}{2\pi}}\langle\langle \exp(-x^2\xi^2)\rangle\rangle \qquad x \in [0, \infty]. \tag{36}$$

Noting that the rhs of equation (35) is monotonically decreasing for $x > 0$, one immediately concludes that the phase boundary for this state is given by $x \to 0$ so $\alpha_c = 2/\pi$ and $b_0 = 1/\pi$, regardless of Q.

For $\tilde{b} > 0$ the region where the retrieval solution exists is found numerically by solving the fixed-point equations (A11)–(A13). The result is shown in figure 5 as the full line. The solution appears continuously. Compared with all other architectures treated in the literature—asymmetrically diluted, layered and fully connected—where the storage capacity is zero for $b \geqslant 1/2$, this is only the case here at finite loading $\alpha = 0$. Because of the tilting of the phase diagram in comparison with the one for the asymmetrically diluted model, as seen already for $Q = 3, 4$, this is no longer the case for non-finite loading. The retrieval state is the global minimum of the free energy in the whole retrieval region.

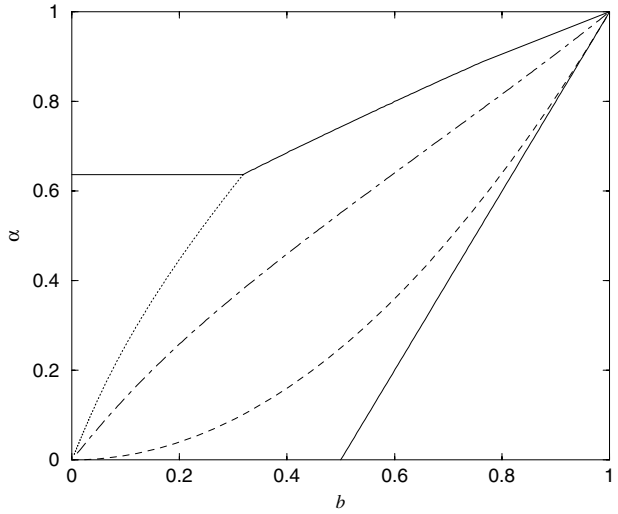

Figure 5. $Q = \infty$ α–b phase diagram at $T = 0$ for uniformly distributed patterns. The short-dashed curve indicates the continuous appearance of the spin-glass state. The meaning of the other curves is as in figures 1 and 2.

For a discussion of the spin-glass phase one can follow a similar argumentation as for the $Q = 3$ model starting from the fixed-point equation analogous to equation (24). One finds that the region of existence of the solution is bounded below by $\alpha \geqslant b^2$, i.e. the dashed curve in figure 5. At the boundary $\chi = 1/b$ and the spin-glass state appears continuously.

In order to determine stability of the retrieval solution against replica symmetry breaking we calculate the replicon eigenvalue using equation (28). The result reads

$$\lambda_R = 1 - \frac{\alpha}{4\tilde{b}^2}\left\langle\!\!\left\langle \int_{|m\xi+\sqrt{\alpha q}z|<2\tilde{b}} \mathcal{D}z \right\rangle\!\!\right\rangle_{\{\xi\}} = 1 - \frac{\alpha\chi}{2\tilde{b}} \tag{37}$$

where we have used the fixed-point equation (A13) for χ. In contrast with the $Q = 3$ model where the replicon eigenvalue is always negative and hence breaking occurs in the whole retrieval region we find that there is only partial breaking here. The AT boundary above which the replicon eigenvalue is positive and, hence, breaking occurs, is shown as the dashed–dotted curve in figure 5.

Finally, we study the $Q = \infty$ model at non-zero temperatures. The retrieval phase is obtained by numerically solving the fixed-point equations (16)–(19). The result is presented as the full line in figure 6. The retrieval state appears continuously and the lower branch of the retrieval boundary ends in zero for $b = 0.5$. For smaller b it crosses the T-axis, e.g. at $T = 1/3$ for $b = 0$.

Next, we find the boundary of the spin-glass phase by expanding the relevant equations (16)–(19) for $m = 0$ with respect to q. We obtain

$$\alpha_{\mathrm{SG}} = \chi_0^{-2} \tag{38}$$

with

$$\begin{aligned} \chi_0 &= \beta \frac{\int_{-1}^{1} \mathrm{d}\sigma\, \sigma^2 \exp(-\beta\tilde{b}_0\sigma^2)}{\int_{-1}^{1} \mathrm{d}\sigma \exp(-\beta\tilde{b}_0\sigma^2)} \\ \tilde{b}_0 &= b - \frac{1}{2\chi_0}. \end{aligned} \tag{39}$$

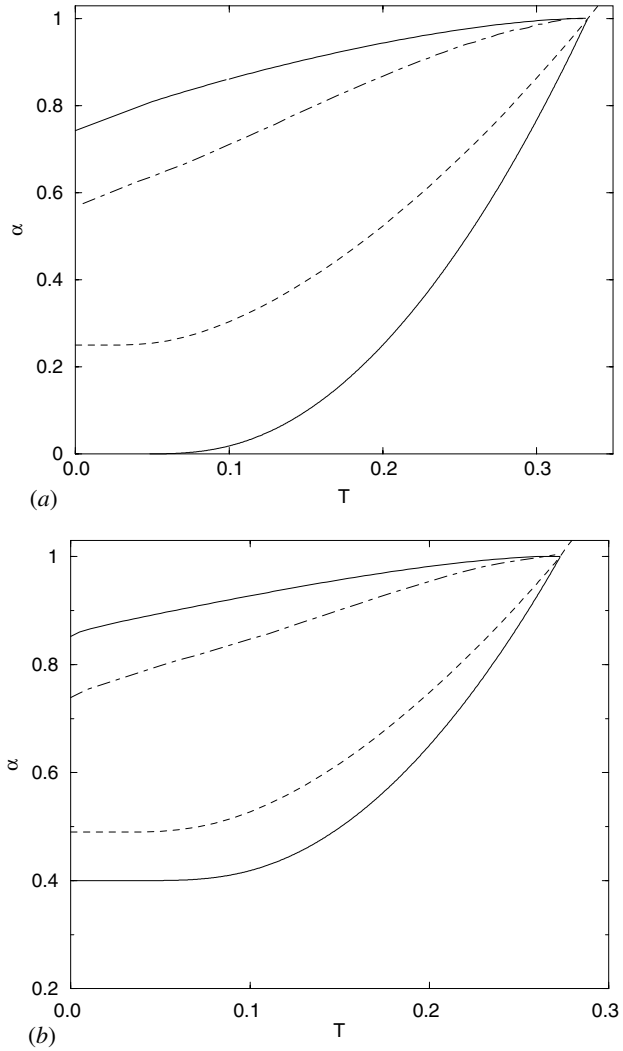

Figure 6. $Q = \infty$ α–T phase diagram for uniformly distributed patterns and (*a*) $b = 0.5$ and (*b*) 0.7. The short-dashed curve indicates the continuous appearance of the spin-glass state. The meaning of the other curves is as in figures 1 and 2.

The result is the short-dashed line in figure 6 above which spin-glass solutions exist.

Concerning the paramagnetic states the same reasoning can be followed as for the $Q = 3$ model after equation (26), leading to one stable solution, $\chi \sim 1/b$, with respect to longitudinal and transverse fluctuations. However, this solution becomes unstable against transverse fluctuations in the spin-glass region.

Comparing the relevant free energies we find that the retrieval states are the global minima in the whole retrieval region. Finally, equation (28) tells us that above the dashed–dotted AT line the replica-symmetric retrieval solution is unstable. Again the whole upper branch of the retrieval boundary lies in this region. Except for the relevant temperature scale these results show some qualitative similarities with the corresponding $Q = 3$ results.

5. Concluding remarks

We have considered both the thermodynamic properties and retrieval properties of *symmetrically* diluted Q-Ising networks. Fixed-point equations have been derived for general temperature and arbitrary Q in the replica-symmetric mean-field approximation. For $Q = 3$, 4 and ∞ capacity–gain parameter diagrams and capacity–temperature phase diagrams have been discussed in detail.

Concerning the capacity–gain parameter diagrams we find that the results are essentially different for odd and even Q. Furthermore, there are interesting similarities with the *asymmetric* extremely diluted versions of the models. In fact, we find that the phase diagram here is tilted towards higher b-values because of the presence of an extended 2-Ising-like region. The critical boundary of this region is independent of Q. Finally, the phase diagram for $Q = 3$ is precisely the same as the one obtained using an exact dynamical approach after requiring that the evolution of the distribution of the local field becomes stationary.

Looking at the α–T phase diagrams we immediately notice the overall qualitatively similar behaviour of the $Q = 3$ and ∞ model. Furthermore the whole upper branch of the retrieval boundary lies in the replica-symmetric unstable region, in contrast with the fully connected model.

Acknowledgments

This work has been supported in part by the Research Fund of the K U Leuven (grant OT/94/9). The authors are indebted to G Jongen and G Massolo for stimulating discussions. One of us (DB) thanks the Fund for Scientific Research—Flanders (Belgium) for financial support.

Appendix

In this appendix we write down explicitly the fixed-point equations (16)–(19) for $Q = 3$, 4 and ∞. For a three-state network with patterns taking the values $0, \pm 1$ with equal probability, one obtains for a retrieval state

$$m = \int \mathrm{D}z V_\beta \left(m + \sqrt{\alpha q} z, \tilde{b} \right) \tag{A1}$$

$$q = \int \mathrm{D}z \left[\tfrac{2}{3} V_\beta^2 \left(m + \sqrt{\alpha q} z, \tilde{b} \right) + \tfrac{1}{3} V_\beta^2 \left(\sqrt{\alpha q} z, \tilde{b} \right) \right] \tag{A2}$$

$$\chi = \frac{1}{\sqrt{\alpha q}} \int \mathrm{D}z z \left[\frac{2}{3} V_\beta \left(m + \sqrt{\alpha q} z, \tilde{b} \right) + \frac{1}{3} V_\beta \left(\sqrt{\alpha q} z, \tilde{b} \right) \right] \tag{A3}$$

where

$$V_\beta(x, y) \equiv \frac{\sinh(\beta x)}{\frac{1}{2} \exp(\beta y) + \cosh(\beta x)}. \tag{A4}$$

For zero temperature the Gaussian variable z can be integrated out explicitly. For $\tilde{b} > 0$ one arrives at

$$m = \frac{1}{2} \left[\operatorname{erf} \left(\frac{m + \tilde{b}}{\sqrt{2\alpha q}} \right) + \operatorname{erf} \left(\frac{m - \tilde{b}}{\sqrt{2\alpha q}} \right) \right] \tag{A5}$$

$$q = 1 - \frac{1}{3} \left[\operatorname{erf} \left(\frac{m + \tilde{b}}{\sqrt{2\alpha q}} \right) - \operatorname{erf} \left(\frac{m - \tilde{b}}{\sqrt{2\alpha q}} \right) + \operatorname{erf} \left(\frac{\tilde{b}}{\sqrt{2\alpha q}} \right) \right] \tag{A6}$$

$$\chi = \sqrt{\frac{2}{9\pi\alpha q}}\left[\exp\left(-\frac{(m+\tilde{b})^2}{2\alpha q}\right)+\exp\left(-\frac{(m-\tilde{b})^2}{2\alpha q}\right)+\exp\left(-\frac{\tilde{b}^2}{2\alpha q}\right)\right]. \tag{A7}$$

For a four-state model in which the patterns can take the value $\pm 1/3, \pm 1$ with equal probability the fixed-point equations (16)–(19) for a retrieval state at zero temperature read

$$m = \frac{3}{10}\left[\operatorname{erf}\left(\frac{3m+\tilde{b}}{3\sqrt{2\alpha q}}\right)+\operatorname{erf}\left(\frac{3m-\tilde{b}}{3\sqrt{2\alpha q}}\right)+\operatorname{erf}\left(\frac{m}{\sqrt{2\alpha q}}\right)\right] + \frac{1}{10}\left[\operatorname{erf}\left(\frac{m+\tilde{b}}{3\sqrt{2\alpha q}}\right)+\operatorname{erf}\left(\frac{m-\tilde{b}}{3\sqrt{2\alpha q}}\right)+\operatorname{erf}\left(\frac{m}{3\sqrt{2\alpha q}}\right)\right] \tag{A8}$$

$$q = 1-\frac{2}{9}\left[\operatorname{erf}\left(\frac{3m+\tilde{b}}{3\sqrt{2\alpha q}}\right)-\operatorname{erf}\left(\frac{3m-\tilde{b}}{3\sqrt{2\alpha q}}\right)+\operatorname{erf}\left(\frac{m+\tilde{b}}{3\sqrt{2\alpha q}}\right)-\operatorname{erf}\left(\frac{m-\tilde{b}}{3\sqrt{2\alpha q}}\right)\right] \tag{A9}$$

$$\chi = \frac{2}{3\sqrt{2\pi\alpha q}}\left[\exp\left(-\frac{(3m+\tilde{b})^2}{18\alpha q}\right)+\exp\left(-\frac{(3m-\tilde{b})^2}{18\alpha q}\right)+\exp\left(-\frac{m^2}{2\alpha q}\right) + \exp\left(-\frac{(m+\tilde{b})^2}{18\alpha q}\right)+\exp\left(-\frac{(m-\tilde{b})^2}{18\alpha q}\right)+\exp\left(-\frac{m^2}{18\alpha q}\right)\right]. \tag{A10}$$

Again, the above expressions are valid only for $\tilde{b} \geqslant 0$.

Finally, for $Q = \infty$ and uniformly distributed patterns ($A = 1/3$) a retrieval state is given by the solution of the fixed-point equations (16)–(18) and (32). For the retrieval state at zero temperature the neuron expectation value $\langle\sigma(z)\rangle = g_{\tilde{b}}(m\xi + \sqrt{\alpha q}z)$, with the effective input–output function $\tilde{g}$ given by (7). This allows us to perform explicitly the Gaussian average in the fixed-point equations resulting in

$$m = \frac{3}{2}\int_{-1}^{1} d\xi\, \xi\left[\left(1+\frac{m\xi}{2\tilde{b}}\right)\operatorname{erf}\left(\frac{2\tilde{b}+m\xi}{\sqrt{2\alpha q}}\right)+\frac{1}{\tilde{b}}\sqrt{\frac{\alpha q}{2\pi}}\exp\left(-\frac{(2\tilde{b}+m\xi)^2}{2\alpha q}\right)\right] \tag{A11}$$

$$q = 1+\frac{1}{2}\int_{-1}^{1} d\xi\left[\left(\frac{\alpha q+(m\xi)^2}{(2\tilde{b})^2}-1\right)\operatorname{erf}\left(\frac{2\tilde{b}+m\xi}{\sqrt{2\alpha q}}\right) + \frac{1}{\tilde{b}}\sqrt{\frac{\alpha q}{2\pi}}\left(\frac{m\xi}{2\tilde{b}}-1\right)\exp\left(-\frac{(2\tilde{b}+m\xi)^2}{2\alpha q}\right)\right] \tag{A12}$$

$$\chi = \frac{1}{4\tilde{b}}\int_{-1}^{1} d\xi \operatorname{erf}\left(\frac{2\tilde{b}+m\xi}{\sqrt{2\alpha q}}\right) \tag{A13}$$

for positive $\tilde{b}$. We remark that it is also straightforward to perform the integration associated with the random patterns but there is no need to write down the resulting expressions.

References

[1] Bollé D, Jongen G and Shim G M 1999 *J. Stat. Phys.* **96** 861
[2] Derrida B, Gardner E and Zippelius A 1987 *Europhys. Lett.* **4** 167
[3] Bollé D, Shim G M, Vinck B and Zagrebnov V A 1994 *J. Stat. Phys.* **74** 565
[4] Watkin T L H and Sherrington D 1991 *Europhys. Lett.* **14** 791
[5] Patrick A E and Zagrebnov V A 1990 *J. Phys. A: Math. Gen.* **23** L1323
Patrick A E and Zagrebnov V A 1992 *J. Phys. A: Math. Gen.* **25** 1009
[6] Watkin T L H and Sherrington D 1991 *J. Phys. A: Math. Gen.* **24** 5427
[7] Rieger H 1990 *J. Phys. A: Math. Gen.* **23** L1273
[8] Canning A and Naef J-P 1992 *J. Physique* I **2** 1791

[9] Viana L and Bray A J 1985 *J. Phys. C: Solid State Phys.* **18** 3037
[10] Bidaux R, Carton J P and Sarma G 1976 *J. Phys. A: Math. Gen.* **9** L87
[11] Bollé D, Rieger H and Shim G M 1994 *J. Phys. A: Math. Gen.* **27** 3411
[12] Mézard M, Parisi G and Virasoro M A 1978 *Spin Glass Theory and Beyond* (Singapore: World Scientific)
[13] Shiino M and Fukai T 1990 *J. Phys. A: Math. Gen.* **23** L1009